ADVANCED OPTICAL MATERIALS
www.advopticalmat.de

Influence of Intermolecular Packing on Light Emitting Efficiency and Carrier-Mobility of Organic Semiconductors: Theoretical Descriptor for Molecular Design

*Qi Sun, Tong Jiang, Qi Ou, Qian Peng, and Zhigang Shuai**

Integration of luminescence and carrier transport is of prime interest for optoelectronics, but full with challenges in organic semiconductors. Previously, it has been demonstrated that intermolecular charge transfer (ICT) in the herringbone H-aggregate can lend oscillator strength to the lowest-lying dark state if electron transfer (t_e) and hole transfer (t_h) integrals are in phase (same sign) and greater than $\sqrt{2}J$, where J is exciton coupling. In this work, both herringbone and π–π stackings are considered and a universal descriptor $I = 2t_e t_h / [(|t_e| + |t_h|)\cdot|J|]$ is proposed. It is found that for π–π stacking with $I > 1$ and for herringbone with $I > \sqrt{2}$, respectively, the lowest dark state could become bright through mixing ICT component. Accordingly, it is found that eclipsed packing and use of molecules with acene-like frontier molecular orbital profiles favor larger I value than the other packing patterns. Finally, with the help of the proposed descriptor, 13 high-mobility emissive unit cores from 32 fused ring molecules are effectively screened out.

1. Introduction

Organic electronics have achieved great success in terms of organic light-emitting diodes (OLEDs),[1] organic field-effect transistors (OFETs),[2] organic solar cells (OSCs),[3] and organic thermoelectrics.[4] Recently, the development of organic light-emitting transistors (OLETs)[5] has attracted increasing attention due to the great potential for the integration of next-generation flexible electronics, electrically pumped organic lasers, and optical communication techniques. OLETs can combine the switching property and current amplification of the OFETs with the light emission of the OLEDs. However, the molecular designs for OLETs materials are rather hindered. This is due to the fact that high mobility is often in contradictory to optical emission for organic semiconductors, because i) the nonradiative decay due to carrier recombination is proportional to mobility,[6] and ii) face-to-face stacking is more favorable for transport but not for optical emission due to H-aggregate formation while head-to-tail is favorable for emission due to J-aggregate but not for transport.[7] Thus, molecular designs for luminescence and mobility are usually carried out separately. Due to the increasing requirements and developing expectations of these portable and multifunctional devices, it is of great interests to develop high mobility and emission materials for OLETs. It should be noted that, despite the above difficulties, significant progresses have been achieved in both the experimental and theoretical aspects. For instance, β-CNDSB[8] has been found to exhibit high photoluminescence quantum yield (PLQY) of 75% with hole and electron mobility (μ) 2.10 and 2.50 $cm^2\ V^{-1}\ s^{-1}$, respectively. DPA[9] possesses superior hole mobility of 34.0 $cm^2\ V^{-1}\ s^{-1}$ with PLQY of 41.3%. And 2-PhVA[10] has a high hole mobility up to 10.0 $cm^2\ V^{-1}\ s^{-1}$. Spano et al. derived charge transfer (CT) induced J- and H-aggregates behavior under the perturbative regime and resonance regime.[11] Based on a three-state model, we provided theoretical insight to make the transport and luminescence compatible taking the herringbone stacking structure as example, within which the intermolecular charge transfer (ICT) could introduce some oscillator strength in the dipole-forbidden lowest exciton state (**Figure 1**a) when the electron transfer (t_e) and hole transfer (t_h) are of the same sign and large than $\sqrt{2}J$.[12] For the 2,6-substituted anthracene derivatives, it was found that the eclipsed stacking pattern is favorable to achieve both high mobility and luminescence[12] (Figure 1b) because the sign of t_e and t_h are generally in phase in this packing motif. Since the interests in pursuing both of the transport and luminescence and the relationship between the packing and properties of the materials, it's of great importance to screen out target high mobility materials effectively

Q. Sun, T. Jiang, Q. Ou, Z. Shuai
MOE Key Laboratory of Organic Optoelectronics and Molecular Engineering
Department of Chemistry
Tsinghua University
Beijing 100084, P. R. China
E-mail: zgshuai@tsinghua.edu.cn

Q. Ou
AI for Science Institute
Beijing 100080, P. R. China

Q. Peng
School of Chemical Sciences
University of Chinese Academy of Sciences
Beijing 100049, P. R. China

Z. Shuai
School of Science and Engineering
The Chinese University of Hong Kong
Shenzhen, Guangdong 518172, P. R. China

The ORCID identification number(s) for the author(s) of this article can be found under https://doi.org/10.1002/adom.202202621.

DOI: 10.1002/adom.202202621

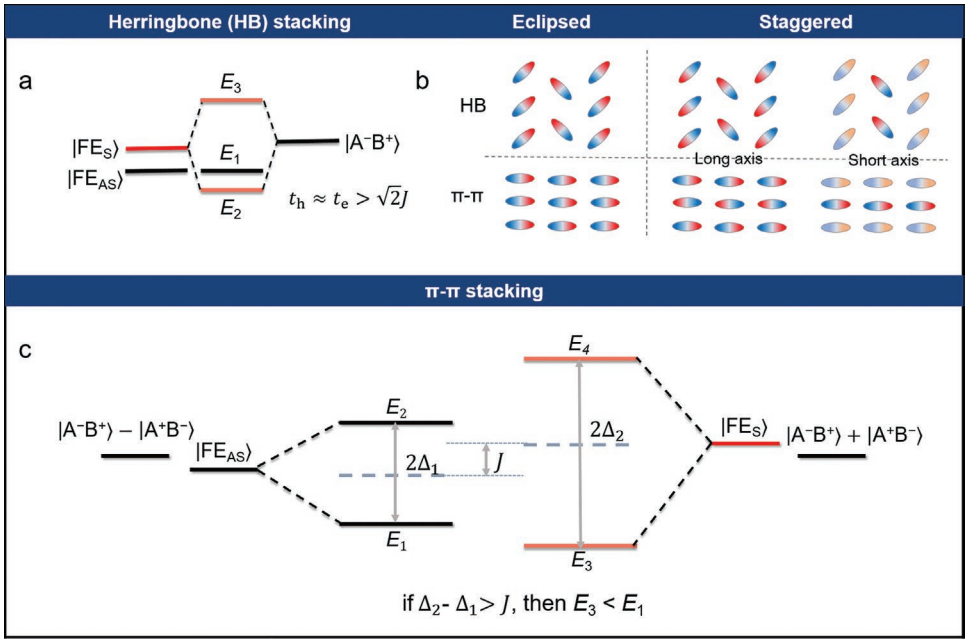

Figure 1. Schematic graph of the ICT induced strong optical emission mechanism in a) herringbone packing (Here A and B denote the monomer) and c) π–π packing H-aggregates. b) Different packing patterns in herringbone packing (top panel) and π–π packing (bottom panel).

and cheaply and favored packing motif through theoretical calculations.

In this paper, four-state model which consist of two local Frenkel excitons and two ICT excitons has been established aiming to clarify the relationship between mobility and luminescence in π–π stacking materials. we propose a universal descriptor I, contributed by intermolecular couplings (J, t_e, and t_h), which is validated through the correlation with experimental measurements. We investigate the relationship between the descriptor I and the different packing geometries for both herringbone and π–π stacking to reveal the structure—property relationship. Finally, we have effectively screened out potential high mobility emissive candidates from 32 materials including both herringbone stacking and π–π stacking fused rings.

2. Results and Discussion

2.1. Four-State Model Hamiltonian and Theoretical Descriptor

Up to now, the documented high mobility materials are all possess herringbone stacking and we have established three-state model for herringbone packing crystals.[12] Beside herringbone stacking, π–π stacking is widely regarded as the most efficient pattern to achieve high carrier mobility. It is highly desirable to derive the condition for both high mobility and high light-emission in such materials. In π–π stacking, a dimer in general possesses two degenerated CT excitons, A^-B^+ and A^+B^-, while the energy degeneracy is generally not preserved in the herringbone structure.[12] Thus, a four-state model Hamiltonian comprising local Frenkel exciton A*B, AB* and ICT exciton A^-B^+, A^+B^- is necessary for π–π stacking and three-state model for herringbone.[12] The formalism of the coupling matrix elements can be found in Supporting Information (SI). The couplings between A*B, AB* and A^-B^+, A^+B^- are recognized as hole transfer integral t_h (A*B and A^-B^+, AB* and A^+B^-) or electron transfer integral t_e (A*B and A^+B^-, AB* and A^-B^+). Thus, the diabatic Hamiltonian is of the form

$$\widehat{H} = \begin{bmatrix} E & J & t_h & t_e \\ J & E & t_e & t_h \\ t_h & t_e & E_{CT} & 0 \\ t_e & t_h & 0 & E_{CT} \end{bmatrix} \quad (1)$$

where E is the excitation energy of S_1 of each monomer; E_{CT} is the excitation energy of A^-B^+ and A^+B^-. We ignore the coupling between the two CT states. The two eigenstates expressed in Frenkel exciton basis and ICT basis are (the other two are shown in supporting information)

$$\Psi_1 = N_1\left[(E_{CT} - E_1)|FE_{AS} - (t_h - t_e)\left(|A^-B^+ - |A^+B^-\right)\right] \quad (2.1)$$

$$\Psi_3 = N_3\left[(E_3 - E_{CT})|FE_S + (t_h + t_e)\left(|A^-B^+ + |A^+B^-\right)\right] \quad (2.2)$$

where the corresponding eigenenergies are

$$E_1 = \frac{1}{2}\left(E_{CT} + E - J - 2\Delta_1\right) \quad (3.1)$$

$$E_3 = \frac{1}{2}\left(E_{CT} + E + J - 2\Delta_2\right) \quad (3.2)$$

where $|FE_{AS}\rangle$ is the asymmetric (dark) state ($|FE_{AS}\rangle = 2^{-\frac{1}{2}}(|A*B\rangle - |B*A\rangle)$). It is noted that Ψ_1 and Ψ_2 are split pair states centered at $\frac{1}{2}(E_{CT}+E-J)$, while Ψ_3 and Ψ_4 are another split pair centered at $\frac{1}{2}(E_{CT}+E+J)$ as shown in Figure 1c, and the latter are bright state with component of $|FE_S\rangle$. If $E_3 < E_1$, then according to Kasha's rule, the optical emission would be allowed. Namely, the split of the latter pair should be large enough to counteract the Frenkel exciton coupling J, which gives rise to a condition $J \le \frac{2t_e t_h}{|t_e + t_h|}$ when $E_{CT} = E + J$. In such case, the energy level ordering follows $E_3 < E_1 < E_4 < E_2$, shown in Figure 1c. Herein, we propose a more general descriptor I which can describe π–π stacking cases:

$$I = \frac{2t_e t_h}{(|t_e| + |t_h|)\cdot|J|} \tag{4}$$

The reason we choose $|t_e| + |t_h|$ not $|t_e + t_h|$ is that when t_e and t_h are of opposite sign, I would be especially negative if we use $|t_e + t_h|$. $|J|$ is used here because in J-aggregates ($J < 0$), t_e and t_h are also needed of the same sign just like H-aggregates. From the results of four-state model, I should be equal to or larger than 1.0 to make the optical emission allowed in π–π stacking cases. The condition is more general since we do not restrict the equal amplitude of t_e and t_h, which is restricted in our previous work for convenience in herringbone materials.[12] And we believe the descriptor could also be used in herringbone materials, which can be viewed as a special case of the four-state model. Since the diagonalization of the parameterized three-state model in herringbone materials are tediously complicated, we conduct model case study to reveal the relationship between the percentage of $|FE_S\rangle$ (ω_{FE_s}) and I as shown in Figure S1 (Supporting Information), it can be seen than when $I > \sqrt{2}$, the emission cannot be totally quenched and could retain at least 50% radiative contribution compared to the monomer emission. And when $E_{CT} > E + J$, the emission could have opportunity to be enhanced (Figure S2, Supporting Information). In fact, by comparing Equation (3.2) with Equation (3.1), it is easily seen that balanced t_e and t_h and higher E_{CT} can very effectively drop E_3 under E_1. This is in accordance with herringbone stacking materials that the couplings of ICT and bright $|FE_S\rangle$ or dark $|FE_{AS}\rangle$ is $\frac{\sqrt{2}}{2}(t_h + t_e)$, $\frac{\sqrt{2}}{2}(t_h - t_e)$, respectively.[19] And with higher E_{CT}, S_1 could borrow more intensity from $|FE_S\rangle$ as seen in Figure S2 (Supporting Information). I could stress the importance of balanced electron and hole transport, namely, when $t_e = t_h$, I is maximized. A negative I value could be obtained when t_e and t_h are of the opposite sign, making I more reasonable that negative I could represent emission forbidden situation. As can be seen from the definition of I, large positive I value necessitate both large and comparable size of t_e and t_h value along with t_e and t_h noticeably larger than J which are required not just by π–π stacking materials, but also by herringbone materials. Even though I does not contain any term about the energy gap of the E and E_{CT}, the effect of it could be reflected by the relatively values of J, t_e and t_h in some extent, as E_{CT} is very sensitive to the distance of the two monomers where E_{CT} is increasing with the longer distance[13] and this would lead to the much more decrease of the values of t_e and t_h (t_e and t_h are matters of wavefunction overlap which show exponentially decay behavior and J show cube decay behavior). That is, the impact of E_{CT} could be reflected by t_e and t_h in some extent. The main difference between herringbone crystal and π–π stacking crystals is the number of ICT state, which making herringbone crystal superior than π–π stacking crystals under $E_{CT} = E + J$ assumption because the percentage of A*B and AB* could be different in herringbone crystals (Figure S3, Supporting Information), resulting less optical emission totally forbidden phenomenon ($\omega_{FE_s} = 0$). While in π–π stacking crystals, the percentage of A*B and AB* are the same, leading to totally quenched luminescence in π–π stacking crystals when $I < 1$ (Figure S1b, Supporting Information). When E_{CT} become higher as seen in Figure S2 (Supporting Information), the requirement of I is also increased, and π–π stacking materials behave more like herringbone materials that appearing partly quenched phenomenon ($0 < 2\omega_{FE_s} < 1$). Thus, we choose $I > 1$ for π–π stacking crystals and $I > \sqrt{2}$ for herringbone crystals as criteria to screen out high performance high mobility emissive materials.

In order to further validate the descriptor I, we plot the I with regard to the experimental value $\sqrt{\mu}\cdot$PLQY of nine literature reported high mobility emissive[8,9,14] crystals as are shown in **Figure 2**a and Table S1 (Supporting Information). The theoretically computed I and experimental $\sqrt{\mu}\cdot$PLQY parameters manifest a compelling linear relationship (Figure 2b), indicating materials with larger I value usually perform better in term of transport luminescence aspect. The reason we choose $\sqrt{\mu}$ not μ is that I is linearly proportional to the transfer integral and μ is proportional to the square of transfer integral. From the results of Figure 2b, only AN,[15] DPA[9] and dNaAnt[14f] satisfy $I > \sqrt{2}$ condition, which is in accordance with experiments that they show enhanced radiative rates from solution to crystal. For the other materials, either their PLQY in solution or the lifetime haven't been reported, so we cannot judge the change of the radiative rates in experiments. But some of them show largely quenched luminescence, such as 2,6-DPSAnt[14b] and AC5[14d] exhibit 0.70 and 0.74 PLQY in solution, while the PLQY in the crystal phase is 0.14 and 0.35, respectively. Moreover, the experimental change of the PLQY from solution to crystal is in accordance with the change of the oscillator strength calculate by optimal range separated functional[16] from monomer to dimer (Table S2, Supporting Information), further validating the model Hamiltonian we use and the descriptor we propose. The diversity of materials we select in Figure 2a is a bit limited because the reported types of high-mobility emissive crystals are quite few with which are generally anthracene derivatives. This would make the descriptor I of the great significance because we could use I to cheaply and effectively screen out potential candidates to enrich the family of high mobility materials. Therefore, a universal descriptor I which could be used to screen out the promising high mobility emissive materials in both of herringbone stacking materials and π–π stacking materials has been established.

2.2. The Relationship between the Descriptor I and the Packing Modes

Transfer integrals strongly depend on the mode of packings[12,17] through the intermolecular overlap between the

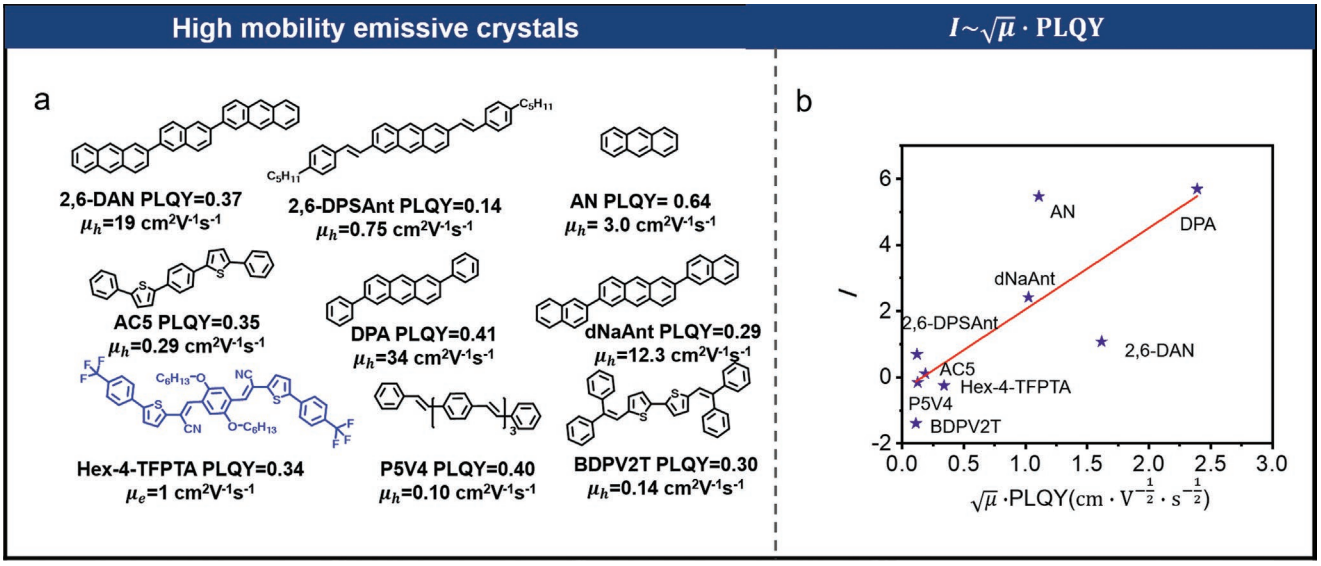

Figure 2. a) High mobility emissive materials and their corresponding PLQY in crystals and mobility measured from transistors (Hex-4-TFPTA in blue is π–π packing, the others are herringbone packing). b) The linear relationship between I and $\sqrt{\mu}$·PLQY, the parameters needed to calculate I are calculated at the ωB97X-D/6-31G(d).

frontier molecular orbitals (MOs): HOMO for hole transfer and LUMO for electron transfer. Thus, the nodal distributions of MOs determine the intermolecular charge transfer integrals. Anthracenes, carbazoles, and fluorenes are frequently employed as either highly emissive or high mobility organic electronic materials.[9,18] Through quantum chemical calculations, we illustrate J, t_e, t_h, and I values as a function of the lateral displacement as shown in Figure S5 (Supporting Information). We are able to classify three types of molecules to reveal the relationship between I and packing geometry: Group I with acene-like frontier orbitals for the compounds such as BTAT,[19] BADT,[20] anthra[2,3-*b*]thiophene[21] and TBTBT2; [22] Group II with carbazole-like frontier orbitals, dibenzo[*b*,*d*]thiophene,[23] BBBT[24] and carbazole as examples; Group III with fluorene-like frontier orbitals, fluorene and EBTT[25] as examples. Each group contains eclipsed herringbone stacking, eclipsed π–π stacking, staggered herringbone stacking, and staggered π–π stacking (Figure 1b). For the eclipsed packing, molecules are aligned in the identical orientation both along the long axis and short axis, whereas in staggered stacking, molecules are arranged in reversed orientation along long axis or short axis. The initial structures are extracted either from crystal or reasonable constructed according to the exist structure in crystal. The results of the relationship between I and different packing motifs as illustrated in Figure 1b are shown in **Figure 3** and Figures S6 and S7 (Supporting Information). It can be seen in Figure 3 that in Group I, the eclipsed packing outperforms the other packing patterns as more packing geometries exhibit I values larger than $\sqrt{2}$ required by herringbone stacking or 1 demanded by π–π stacking. Staggered stacking behaves worse not only in herringbone staking, but also in π–π stacking. While in Group II (Figure S6, Supporting Information), staggered herringbone packing performs better than eclipsed herringbone packing, and both eclipsed and staggered π–π stackings are favorable since for most of the packing geometries, the value of descriptor I always large than 1. As far as Group III is concerned (Figure S7, Supporting Information), very few packing geometries are found to meet the requirement for I. In fact, the signs of t_e and t_h are often opposite and imbalanced and J is usually larger than t_e and t_h. Thus, it can be concluded that *molecules with acene-like frontier MOs in conjunction with eclipsed packing mode or molecules with carbazole-like frontier MOs in π–π stacking are more likely to achieve both high mobility and high luminescence*. In herringbone stacking, we also investigate the relationship between I and herringbone angle as seen in Figures 3, and Figures S8 and S9 (Supporting Information). Compared with lateral displacements, I is less sensitive to the stacking angle. The same conclusion could be drawn that eclipsed herringbone packing in acene-like nodes molecules and π–π stacking in carbazole-like materials are favored in terms of transport and luminescence.

2.3. Screening out Molecules with high Mobility and Emission from Fused Ring Compounds

Fused ring compounds often serve as building block or unit core for high luminescence or high mobility materials. For instance, anthracene (**1**) shows 0.24 PLQY in solution and enhanced 0.64 PLQY in crystal and 3 cm^{2}V^{-1}s^{-1} mobility for single-crystal OFET device.[15] Carbazole (4) and BTBT[26] (**14**) are well documented high luminescence or high mobility building blocks. NDT (**13**), ABT (**19**), ADT (**24**), DNTT (**29**) and BTAT (**30**) are good transport materials with high mobility.[19,27] Our theoretical design strategy is to computationally screen out high PLQY compounds through calculating the molecular descriptor I. We consider 32 fused ring compounds (**Figure 4**a), including 3-ring fused molecules **1**–**8**, 4-ring fused molecules **9**–**16**, 5-ring molecules **17**–**28** and 6-ring molecules **29**–**32**. The crystal structures are obtained from Cambridge Crystallographic Data Centre

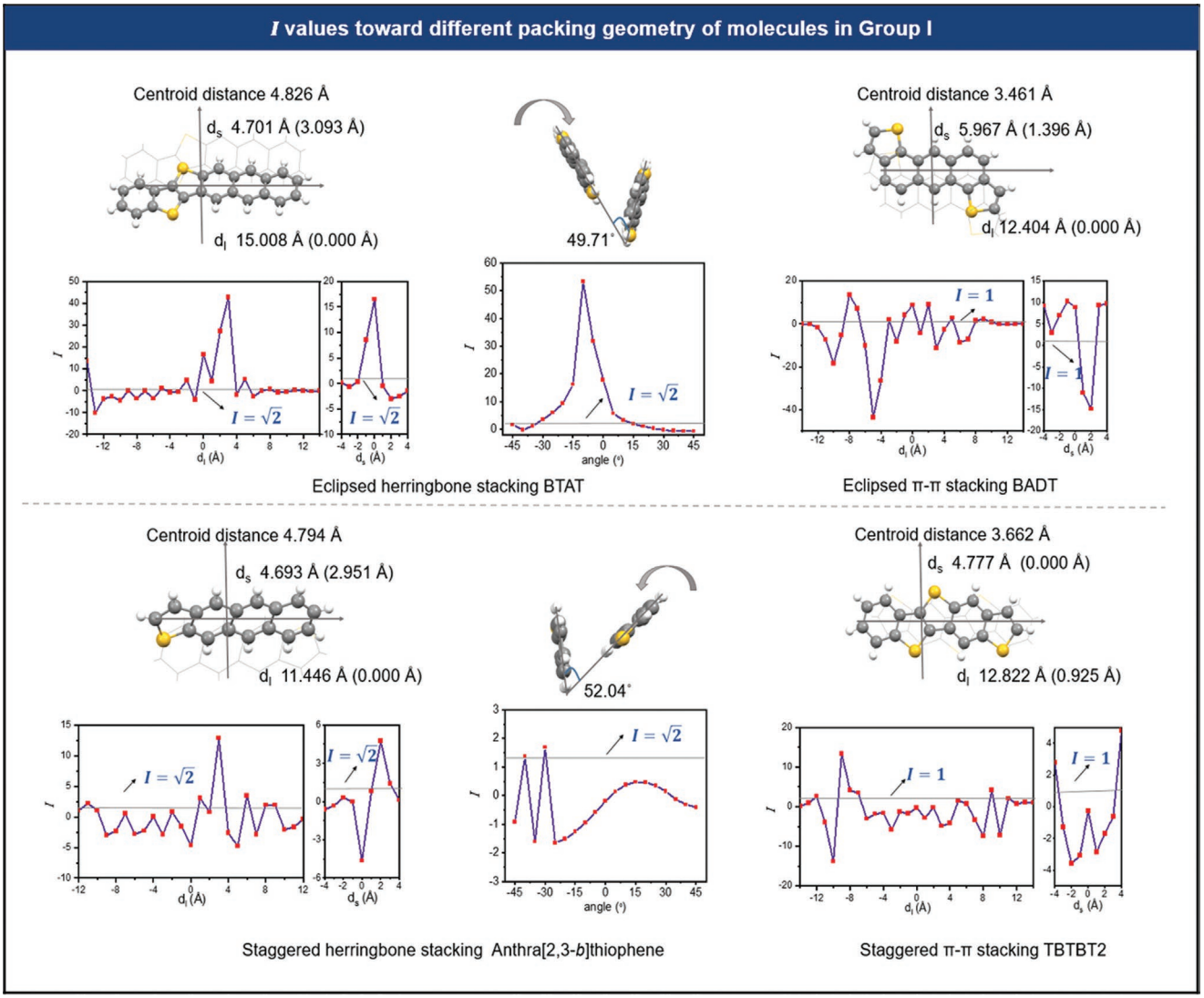

Figure 3. Evolution of *I* as a function of intermolecular lateral displacement along both long and short axis as well as the stacking angle for BTAT, BADT, anthra[2,3-*b*]thiophene and TBTBT2 in Group I for both herringbone and π–π stackings, the parameters needed to calculated *I* are computed at the level of ωB97X-D/6-31G(d). The rotate molecule and the direction of rotation are denoted by the arrow.

(CCDC) with the corresponding structure number shown in Tables S1–S3 (Supporting Information). Here we exclude tetracene and pentacene because the intersystem crossing (ISC) from S_1 to triplet states and singlet fission process lead to the dominant nonradiative decay resulting in weak PLQY in crystalline tetracene and absence of fluorescence in pentacene.[28] Most of the selected moieties are good transport materials, but the PLQYs are rarely documented. The 32 fused-ring compounds were classified into three groups according to their MO nodal distribution patterns. Group I: **1**, **2**, **9**, **10**, **11**, **12**, **13**, **14**, **15**, **17**, **19**, **21**, **23**, **24**, **26**, **29**, **30** all contain acene-like frontier orbital nodal structure. Group II: **4**, **6**, **8**, **18**, **22**, **28** are all with carbazole-like frontier orbitals. And for Group III: **3**, **5**, **7**, **16**, **20**, **25**, **27**, **31**, **32** are all with fluorene-like MOs. The frontier MO and packing pattern are shown in Figure S10 (Supporting Information). The calculated *I* values for the 32 fused rings are provided in Figures 4b and Figure S10 (Supporting Information) and the tabulated values are given in Table S3 (Supporting Information). All of the eclipsed packing molecules in Group I satisfy the high mobility emissive condition defined by *I* descriptor ($I > \sqrt{2}$ in herringbone crystals and $I > 1$ in π–π stacking crystals). Whereas, only one staggered herringbone **14**[29] (BTBT) possesses *I* value larger than $\sqrt{2}$, which is in accordance with our previous work[12] and above discussion. All the other staggered stacking materials fail to fulfill the criteria owing to either the opposite sign of t_e and t_h value (**9**,[30] **12**,[21] **15**,[31] and **26**[22]) or the largely imbalanced t_e and t_h (**10**,[32] and **17**[33]). The promising candidates are herringbone stacking molecules **1**[15] (anthracene, $I = 5.47$), **2**[34] (1*H*-benzo[*f*]indole, $I = 3.73$), **11**[35] (benzo[*b*]naphtho[2,3-*d*]thiophene, $I = 5.93$), **13** (NDT, $I = 13.34$),[36] **14**[29] (BTBT, $I = 1.72$), **19**[27d] (ABT, $I = 11.56$), **24**[37] (ADT, $I = 6.26$), **29**[27a] (DNTT, $I = 2.91$), **30**[19] (BTAT, $I = 16.50$) in Group I and eclipsed π–π stacking materials **21**[38] (ATT, $I = 1.20$), and **23**[20] (BADT, $I = 8.87$) in Group I. In Figure 4c, we

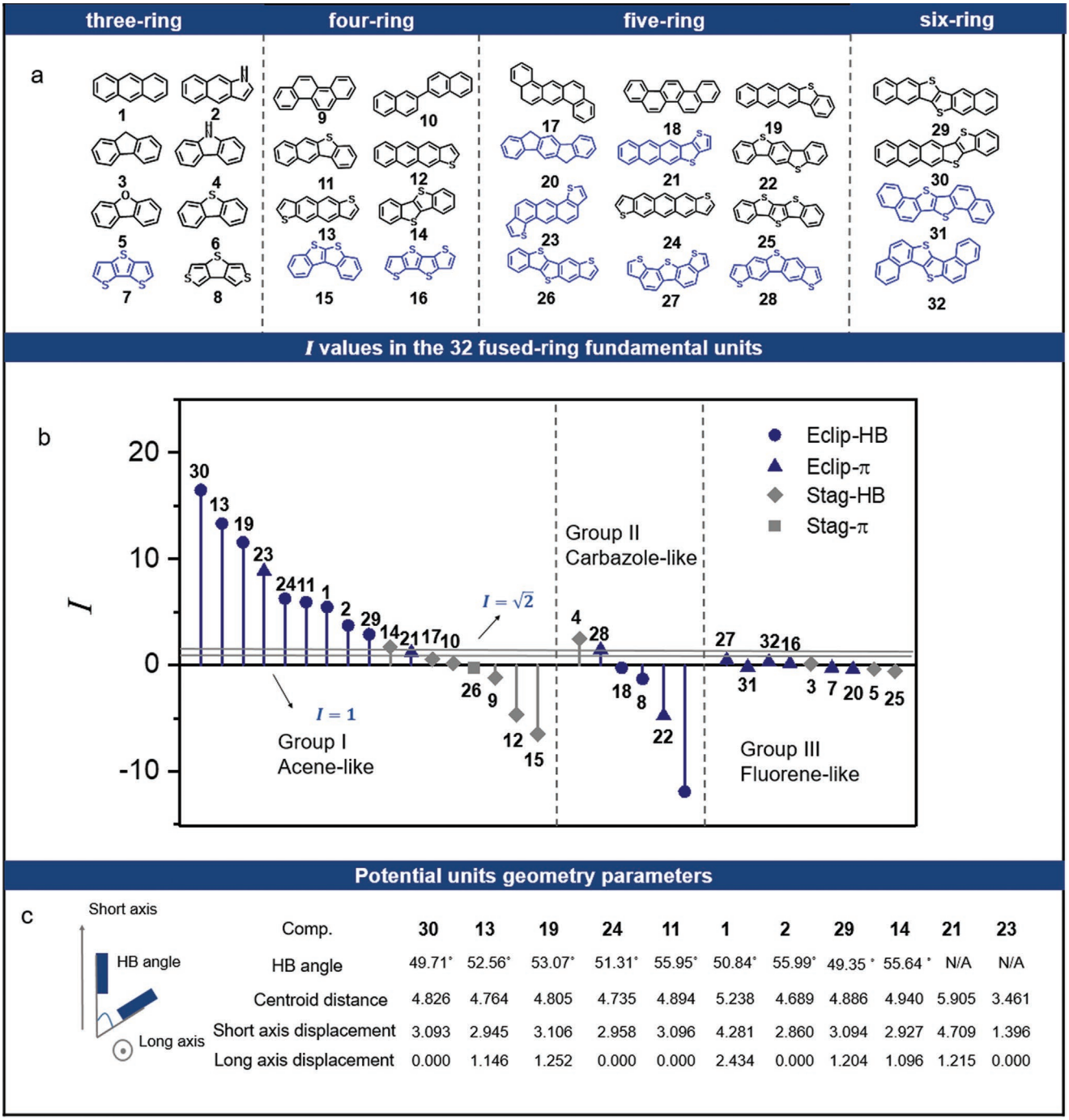

Comp.	30	13	19	24	11	1	2	29	14	21	23
HB angle	49.71°	52.56°	53.07°	51.31°	55.95°	50.84°	55.99°	49.35°	55.64°	N/A	N/A
Centroid distance	4.826	4.764	4.805	4.735	4.894	5.238	4.689	4.886	4.940	5.905	3.461
Short axis displacement	3.093	2.945	3.106	2.958	3.096	4.281	2.860	3.094	2.927	4.709	1.396
Long axis displacement	0.000	1.146	1.252	0.000	0.000	2.434	0.000	1.204	1.096	1.215	0.000

Figure 4. a) Molecular structures of the fused rings investigated in this work. π–π stackings are indicated in blue and the rest are herringbone packing. b) The calculated *I* values for the 32 fused rings. c) Geometric structure parameters of fused rings in Group I which satisfy the high mobility and emission conditions defined by *I* descriptor.

list the geometric structure parameters of the potential fundamental units in Group I. Nine of the herringbone stackings possess quite similar herringbone (HB) angles (in the range of 49.35° to 55.99°) and centroid distance (from 4.689 Å to 4.826 Å and 5.238 Å in **1** because of the longer displacements). In fact, as inferred from Figure 3, the geometric structure parameters for **30**, **13**, **19**, **24**, **11**, **1**, **2**, **29** and **14** fall well in the regime of $I > \sqrt{2}$ and for **21** and **23** in the $I > 1$ regime. From Table S3 (Supporting Information), the t_e and t_h for these compounds are not only of the same sign and balanced values, but also noticeably greater than *J*. The excitonic coupling *J* is proportional to the molecular oscillator strength *f*. Therefore, large *J* is likely to be induced by large *f*. According to Figure S11 (Supporting Information), *J* tends to be larger in the molecules with

three or more thiophene subunits or in the armchair arrangement, which would make I values difficult to be larger than 1 or $\sqrt{2}$. Thus, for the N-fused ring molecules when $N \geq 4$, we recommend the fused ring with one or two five-membered heterocyclic rings in zigzag arrangement. For Groups II and III, only staggered herringbone stacking **4** (carbazole, $I = 2.48$) and eclipsed π–π stacking **28**[39] (thieno[2,3-*f*:5,4-*f* ′]bis[1]benzothiophene, $I = 1.45$) in Group II satisfy the criterion for I, which is consistent with our above discussion. Thus, the descriptor I constructed from model Hamiltonian could demonstrate the relationship between the packing modes and luminescence transport property as well as effectively and cheaply screen out high mobility emissive candidates.

3. Conclusion

To conclude, we have unraveled the mechanism of intermolecular CT induced high luminescence and high carrier mobility for both herringbone and π–π stacking materials using mixed Frenkel-CT exciton models. Then, we proposed a universal descriptor I containing intermolecular couplings (J, t_e, and t_h). We have demonstrated the dependence of I on the molecular packings with respect to lateral displacement along different axis and orientation angles. We are able to identify three types of stacking geometries behaviors related to the frontier molecular orbitals: acene-like, carbazole-like, and fluorene-like. It is found that materials with acene-like frontier orbital nodes and eclipsed packing are the best combination to achieve high mobility and high luminescence simultaneously. Finally, we employ the molecular descriptor to screen out thirteen potential candidates with high PLQY out of 32 high-mobility fused ring compounds through computational studies. The selected fused ring moieties could serve as unit cores to construct novel candidates to enrich the types of high mobility emissive materials. The proposed descriptor I can be straightforwardly evaluated for most materials and is easy to be calculated, which would boost the aperture of OLETs materials in an effective and low-cost way. Especially, it will play essential role for machine-learning based high-throughput screening strategy for designing OLETs materials.

Supporting Information

Supporting Information is available from the Wiley Online Library or from the author.

Acknowledgements

This work was supported by the National Natural Science Foundation of China Grant Nos. 21788102 and 22003030, as well as by the Ministry of Science and Technology of China through the National Key R&D Plan, Grant No. 2017YFA0204501. Q.O. is also funded by China Postdoctoral Science Foundation Grant No. 2020M670280.

Conflict of Interest

The authors declare no conflict of interest.

Data Availability Statement

The data that support the findings of this study are available from the corresponding author upon reasonable request.

Keywords

descriptor, high mobility, packing geometry, photoluminescence quantum yield

Received: November 10, 2022
Published online: December 19, 2022

[1] a) Z. Y. Yang, Z. Mao, Z. L. Xie, Y. Zhang, S. W. Liu, J. Zhao, J. R. Xu, Z. G. Chi, M. P. Aldred, *Chem. Soc. Rev.* **2017**, *46*, 915; b) T. Chiba, Y. J. Pu, J. Kido, *Adv. Mater.* **2015**, *27*, 4681.
[2] C. L. Wang, H. L. Dong, L. Jiang, W. P. Hu, *Chem. Soc. Rev.* **2018**, *47*, 422.
[3] Inganäs, O. , *Adv. Mater.* **2018**, *30*, 1800388.
[4] R. Liu, Y. Ge, D. Wang, Z. Shuai, **2021**, *3*, 1477.
[5] a) R. Capelli, S. Toffanin, G. Generali, H. Usta, A. Facchetti, M. Muccini, *Nat. Mater.* **2010**, *9*, 496; b) C. Zhang, P. Chen, W. Hu, *Small* **2016**, *12*, 1252; c) D. Yuan, V. Sharapov, X. Liu, L. Yu, *ACS Omega* **2020**, *5*, 68; d) S. K. Park, J. H. Kim, T. Ohto, R. Yamada, A. O. F. Jones, D. R. Whang, I. Cho, S. Oh, S. H. Hong, J. E. Kwon, J. H. Kim, Y. Olivier, R. Fischer, R. Resel, J. Gierschner, H. Tada, S. Y. Park, *Adv. Mater.* **2017**, *29*, 1701346; e) M. Zambianchi, E. Benvenuti, C. Bettini, C. Zanardi, R. Seeber, D. Gentili, M. Cavallini, M. Muccini, V. Biondo, C. Soldano, G. Generali, S. Toffanin, M. Melucci, *J. Mater. Chem. C* **2016**, *4*, 9411; f) E. Orgiu, P. Samori, *Adv. Mater.* **2014**, *26*, 1827; g) M. U. Chaudhry, K. Muhieddine, R. Wawrzinek, J. Sobus, K. Tandy, S. C. Lo, E. B. Namdas, *Adv. Funct. Mater.* **2019**, *30*, 1905282; h) Y. Wan, J. Deng, W. Wu, J. Zhou, Q. Niu, H. Li, H. Yu, C. Gu, Y. Ma, *ACS Appl. Mater. Interfaces* **2020**, *12*, 43976; i) Z. Qin, H. Gao, H. Dong, W. Hu, *Adv. Mater.* **2021**, *33*, 2007149.
[6] P. Langevin, *Ann. Chim. Phys.* **1903**, *28*, 433.
[7] C. Wang, H. Dong, W. Hu, Y. Liu, D. Zhu, *Chem. Rev.* **2012**, *112*, 2208.
[8] J. Deng, Y. Xu, L. Liu, C. Feng, J. Tang, Y. Gao, Y. Wang, B. Yang, P. Lu, W. Yang, Y. Ma, *Chem. Commun.* **2016**, *52*, 2370.
[9] J. Liu, H. Zhang, H. Dong, L. Meng, L. Jiang, L. Jiang, Y. Wang, J. Yu, Y. Sun, W. Hu, A. J. Heeger, *Nat. Commun.* **2015**, *6*, 10032.
[10] F. Qiu, Y. Dong, J. Liu, Y. Sun, H. Geng, H. Zhang, D. Zhu, X. Shi, J. Liu, J. Zhang, S. Ai, L. Jiang, *J. Mater. Chem. C* **2020**, *8*, 6006.
[11] a) N. J. Hestand, F. C. Spano, *Acc. Chem. Res.* **2017**, *50*, 341; b) N. J. Hestand, F. C. Spano, *Chem. Rev.* **2018**, *118*, 7069; c) H. Yamagata, C. M. Pochas, F. C. Spano, *J. Phys. Chem. B* **2012**, *116*, 14494.
[12] Q. Sun, J. Ren, T. Jiang, Q. Peng, Q. Ou, Z. Shuai, *Nano. Lett.* **2021**, *21*, 5394.
[13] F. Gao, F. Pan, Y. Zhao, W. Liang, *J. Phys. Chem. B* **2009**, *113*, 14581.
[14] a) L. Zheng, J. Li, K. Zhou, X. Yu, X. Zhang, H. Dong, W. Hu, *Nano Res.* **2020**, *13*, 1976; b) A. Dadvand, W.-H. Sun, A. G. Moiseev, F. Bélanger-Gariépy, F. Rosei, H. Meng, D. F. Perepichka, *J. Mater. Chem. C* **2013**, *1*, 2817; c) S. Ma, K. Zhou, M. Hu, Q. Li, Y. Liu, H. Zhang, J. Jing, H. Dong, B. Xu, W. Hu, W. Tian, *Adv. Funct. Mater.* **2018**, *28*, 1802454; d) Y. Yomogida, T. Takenobu, H. Shimotani, K. Sawabe, S. Z. Bisri, T. Yamao, S. Hotta, Y. Iwasa, *Appl. Phys. Lett.* **2010**, *97*, 173301; e) H. Nakanotani, M. Saito, H. Nakamura, C. Adachi, *Appl. Phys. Lett.* **2009**, *95*, 103307; f) J. Li, K. Zhou, J. Liu, Y. Zhen, L. Liu, J. Zhang, H. Dong, X. Zhang, L. Jiang, W. Hu,

J. Am. Chem. Soc. **2017**, *139*, 17261; g) S. Oh, J. H. Kim, S. K. Park, C. H. Ryoo, S. Y. Park, *Adv. Opt. Mater.* **2019**, *7*, 1901274; h) K. Niimi, H. Mori, E. Miyazaki, I. Osaka, H. Kakizoe, K. Takimiya, C. Adachi, *Chem. Commun.* **2012**, *48*, 5892.

[15] R. Katoh, K. Suzuki, A. Furube, M. Kotani, K. Tokumaru, *J. Phys. Chem. C* **2009**, *113*, 2961.

[16] T. Stein, L. Kronik, R. Baer, *J. Am. Chem. Soc.* **2009**, *131*, 2818.

[17] a) P. M. Kazmaier, R. Hoffmann, *J. Am. Chem. Soc.* **1994**, *116*, 9684; b) V. Coropceanu, J. Cornil, D. A. S. da Filho, Y. Olivier, R. Silbey, J. Bre´das, *Chem. Rev.* **2007**, *107*, 926.

[18] a) K. Takimiya, H. Ebata, K. Sakamoto, T. Izawa, T. Otsubo, Y. Kunugi, *J. Am. Chem. Soc.* **2006**, *128*, 12604; b) P. Rajamalli, N. Senthilkumar, P. Y. Huang, C. C. Ren-Wu, H. W. Lin, C. H. Cheng, *J. Am. Chem. Soc.* **2017**, *139*, 10948; c) L. S. Cui, H. Nomura, Y. Geng, J. U. Kim, H. Nakanotani, C. Adachi, *Angew. Chem., Int. Ed.* **2017**, *56*, 1571; d) I. D. Samuel, G. A. Turnbull, *Chem. Rev.* **2007**, *107*, 1272; e) D. Liu, J. De, H. Gao, S. Ma, Q. Ou, S. Li, Z. Qin, H. Dong, Q. Liao, B. Xu, Q. Peng, Z. Shuai, W. Tian, H. Fu, X. Zhang, Y. Zhen, W. Hu, *J. Am. Chem. Soc.* **2020**, *142*, 6332.

[19] T. Mori, T. Nishimura, T. Yamamoto, I. Doi, E. Miyazaki, I. Osaka, K. Takimiya, *J. Am. Chem. Soc.* **2013**, *135*, 13900.

[20] A. Pietrangelo, M. J. MacLachlan, M. O. Wolf, B. O. Patrick, *Org. Lett.* **2007**, *9*, 3571.

[21] F. Valiyev, W. S. Hu, H. Y. Chen, M. Y. Kuo, I. Chao, Y. T. Tao, *Chem. Mater.* **2007**, *19*, 3018.

[22] Y. Dong, H. Li, J. Liu, J. Zhang, X. Shi, Y. Shi, C. Li, Z. Liu, T. Li, L. Jiang, *Org. Electron.* **2020**, *77*, 105537.

[23] R. M. Schaffri, J. Trotter, *J. Chem. Soc. A* **1970**, *0*, 1561.

[24] P. Gao, D. Beckmann, H. N. Tsao, X. Feng, V. Enkelmann, W. Pisula, K. Mullen, *Chem. Commun.* **2008**, 1548.

[25] K. Mitsudo, H. Sato, A. Yamasaki, N. Kamimoto, J. Goto, H. Mandai, S. Suga, *Org. Lett.* **2015**, *17*, 4858.

[26] K. Takimiya, I. Osaka, T. Mori, M. Nakano, *Acc. Chem. Res.* **2014**, *47*, 1493.

[27] a) T. Yamamoto, K. Takimiya, *J. Am. Chem. Soc.* **2007**, *129*, 2224; b) M. Nakano, H. Mori, S. Shinamura, K. Takimiya, *Chem. Mater.* **2011**, *24*, 190; c) J. G. Laquindanum, H. E. Katz, A. J. Lovinger, *J. Am. Chem. Soc.* **1998**, *120*, 664; d) C. Y. Du, Y. L. Guo, Y. Q. Liu, W. F. Qiu, H. J. Zhang, X. Gao, Y. Liu, T. Qi, K. Lu, G. Yu, *Chem. Mater.* **2008**, *20*, 4188.

[28] a) N. Geacintov, M. Pope, F. Vogel, *Phys. Rev. Lett.* **1969**, *22*, 593; b) X. Ye, Y. Liu, Q. Han, C. Ge, S. Cui, L. Zhang, X. Zheng, G. Liu, J. Liu, D. Liu, X. Tao, *Chem. Mater.* **2018**, *30*, 412; c) T. C. Wu, N. J. Thompson, D. N. Congreve, E. Hontz, S. R. Yost, T. Van Voorhis, M. A. Baldo, *Appl. Phys. Lett.* **2014**, *104*, 193901.

[29] C. Niebel, Y. Kim, C. Ruzié, J. Karpinska, B. Chattopadhyay, G. Schweicher, A. Richard, V. Lemaur, Y. Olivier, J. Cornil, A. R. Kennedy, Y. Diao, W.-Y. Lee, S. Mannsfeld, Z. Bao, Y. H. Geerts, *J. Mater. Chem. C* **2015**, *3*, 674.

[30] S. Banerjee, S. Sinha, P. Pradhan, A. Caruso, D. Liebowitz, D. Parrish, M. Rossi, B. Zajc, *J. Org. Chem.* **2016**, *81*, 3983.

[31] A. Matsunaga, Y. Ogawa, S. Tamura, K. Yamamoto, H. Katagiri, *ChemistrySelect* **2021**, *6*, 4506.

[32] W. G. Chen Minqin, Z. Shanming, H. Zuen, Q. Wenjie, W.u Wenling, *Gaodeng Xuexiao Huaxue Xuebao* **1987**, *8*, 556.

[33] C. H. M. John Iball, D. E. Zacharias, *J. Chem. Soc., Perkin Trans.2* **1975**, 1271.

[34] C. Chen, Z. Chi, K. C. Chong, A. S. Batsanov, Z. Yang, Z. Mao, Z. Yang, B. Liu, *Nat. Mater.* **2021**, *20*, 175.

[35] D. Tian, W. Zhang, G. Shi, S. Luo, Y. Chen, W. Chen, H. Huang, S. Xing, B. Zhu, *Org. Chem. Front.* **2021**, *8*, 4124.

[36] I. Osaka, S. Shinamura, T. Abe, K. Takimiya, *J. Mater. Chem. C* **2013**, *1*, 1297.

[37] M. Mamada, H. Katagiri, M. Mizukami, K. Honda, T. Minamiki, R. Teraoka, T. Uemura, S. Tokito, *ACS Appl. Mater. Interfaces* **2013**, *5*, 9670.

[38] Y. Ogawa, K. Yamamoto, C. Miura, S. Tamura, M. Saito, M. Mamada, D. Kumaki, S. Tokito, H. Katagiri, *ACS Appl. Mater. Interfaces* **2017**, *9*, 9902.

[39] B. Wex, B. R. Kaafarani, K. Kirschbaum, D. C. Neckers, *J. Org. Chem.* **2005**, *70*, 4502.